JOURNAL OF THERMOPHYSICS AND HEAT TRANSFER
Vol. 23, No. 1, January–March 2009

Foam, Fin, and Nanoparticle Thermal Management of Power Amplifiers Using Liquid Cooling

Z. A. Williams*
Miltec Research and Technology, Oxford, Mississippi 38655
and
J. A. Roux†
University of Mississippi, University, Mississippi 38677

DOI: 10.2514/1.39497

This work explores several variations of a liquid-cooled base-plate channel design for a high-packing-spacing array of generic power-amplifier units. Several different channel-insert configurations are investigated as mini heat exchangers using graphite foam, copper fins, or nanoparticles dispersed within the cooling fluid. Experiments were conducted measuring the chip temperatures as a means of determining the effectiveness of the various cooling schemes. Computational fluid dynamics simulations were also conducted to guide the experimental program. Effective heat transfer coefficients were also reverse-engineered using computational fluid dynamics software and the experimental results. The results presented are useful for thermal designers seeking effective thermal-management alternatives that may be most effective for a given application.

I. Introduction

THERMAL design plays a crucial role in the design of electronic-systems that can manage dissipated thermal heat and channel it to flow from the heat source to the ambient environment [1]. An increase in the demand on electronic-system performance and reliability, as well as a movement toward the miniaturization of circuits and arrays, has heightened the demand for more innovative methods of thermal control. Miniaturization of circuits has decreased the size of individual electronic components, but has conversely increased the number of components that can be integrated onto a single chip. This and a progression toward large-scale chip integration have lead to a significant increase in chip-dissipated heat fluxes [2,3]. These increasing demands in performance have created the requirement for thermal designs that can manage temperatures within the system to operate below the failure temperature (150°C).

A wide variety of approaches are being applied to electronic systems to manage the high levels of thermal power that must be accommodated. Forced-air convection cooling of systems has been popular since the early 1990s, mostly due to their simplicity and cost-effectiveness [3,4]. Base-plate channel cooling, with several options of cooling fluids, is another applicable cooling method for electronic systems [5,6]. Although more sophisticated and costly, systems incorporating liquid cooling are necessary to meet the demands of many high-heat-flux applications [7–9]. For situations in which space management is important, such as notebook computers, heat pipes are well suited [10]. In recent years, there has also been some investigation into the performance of nanofluids for the cooling of electronics [11].

With many cooling-approach choices, it is necessary that each cooling system be investigated on an individual basis. Computer simulation has become an invaluable tool for enhancing thermal management for specific applications. Thermal engineers frequently use computational fluid dynamics (CFD) software in the electronics industry to evaluate and adapt cooling designs to their application.

The current work uses CFD simulations as a guide to experimental simulations to develop a thermal-management system for an array of power-amplifier units, with the emphasis on the experimental testing. The proposed experimental design employs base-plate channel cooling with water as the cooling fluid. A previous companion study [12] using air as the cooling fluid showed that the use of various cooling mechanisms significantly reduced the power-amplifier chip temperatures by as much as 47°C or more. The present work is a follow-up experimental study to explore some of the same [12] and some different cooling mechanisms but with water as the cooling fluid.

For the present investigation, three heat-transfer-enhancing materials (carbon graphite foam, copper fins, or nanoparticles) were placed in the cooling channel of the base plate to function as mini heat exchangers and enhance the convective heat transfer in the cooling channel. Carbon graphite foam used in the current study was pyrolytic foam with an open cell structure that yields a large surface area and high porosity, which enhances the convective heat transfer [13,14]. Aluminum-oxide (Al_2O_3) or copper oxide (CuO) nanoparticles were dispersed at various volume percentages within the cooling fluid to determine their effectiveness in comparison with the graphite foams and copper fins. The overall objective of this study is to determine/quantify the amount of improvement in thermal management by graphite foam, copper fins, or nanoparticles with water as the cooling fluid as opposed to air [12] as the cooling fluid.

II. Statement of the Problem

The goal of the present study is the thermal management of an array of power-amplifier units. The power-amplifier unit of interest in the current study consists of an aluminum nitride substrate that is populated with chips and circuitry. A cover encloses the electronics to protect the chips from environmental elements. Each unit has seven chips of varying sizes and power-dissipation levels. One of these chips, the *power chip*, has a much higher dissipated thermal power than the other six chips and is therefore the critical component and the focus of the current study. Successfully managing the temperature of the power chip on each unit is essential to the proper operation of the entire system array. The maximum allowable temperature for the power chip is 150°C; therefore, electronic failure is considered to occur at temperatures above 150°C.

Here, four units are mounted side by side on a copper base plate and will be referred to as a *stick*. Figure 1 illustrates this with the

Presented as Paper 4251 at the 40th Thermophysics Conference, Seattle, WA, 23–26 June 2008; received 2 July 2008; revision received 29 September 2008; accepted for publication 1 October 2008.

*Engineer, 9 Industrial Park Drive, Suite 101.
†Faculty, Mechanical Engineering, Carrier Hall, Room 201H. Associate Fellow AIAA.

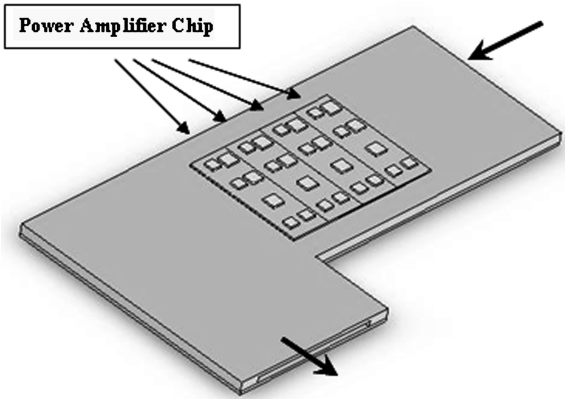

Fig. 1 Water-cooled base plate (top) with substrates and chips.

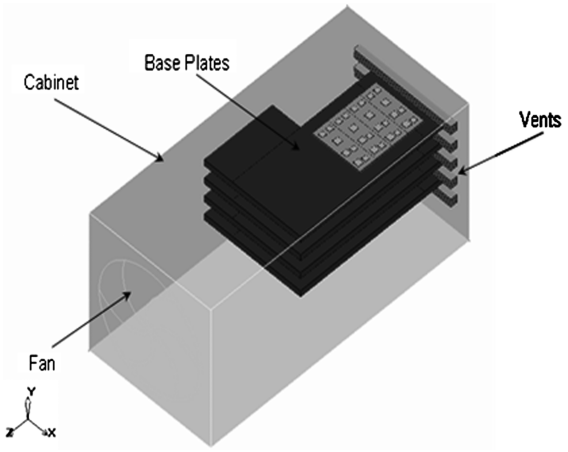

Fig. 2 IcePak sketch of water-cooled design.

covers removed from the modules, exposing the chips. A cooling channel is located directly under the amplifier units. Water is forced through this channel at various flow rates: [1.58×10^{-5} m^3/s (0.25 gpm), 3.15×10^{-5} m/s, and 6.31×10^{-5} m^3/s (1.00 gpm)]. Fluid flowing through the channel removes the heat dissipated by the power chips through forced convection. The sticks are mounted in a cabinet to isolate them from the environment. As depicted in Fig. 2, the overall array contains 16 (4×4) power-amplifier units; there are 4 sticks mounted in the cabinet, with each stick containing 4 units.

The array has a packing density of 0.020 m; this is the distance from the bottom of one base plate to the bottom of the next adjacent base plate, with an air gap between sticks of 0.009 m. This dimension is dictated by the electrical characteristics of the system and must be maintained to ensure proper electrical operation.

In the present work, several materials were investigated to determine their capability to enhance the heat transfer inside the cooling channel of the base plate. These materials were inserted into the cooling channel directly under the units. Three geometric configurations (inline, corrugated, and zigzag) of two types [POCO and POCO high thermal conductivity (HTC)] of graphite foam, two (zigzag and inline) configurations of copper fins, and two types (Al_2O_3 and CuO) of nanoparticles dispersed within the fluid were investigated.

An improved process of graphitizing carbon foam was developed at Oak Ridge National Laboratories (ORNL), and this process has been licensed to POCO Graphite, Inc. [13]. Three different configurations of graphite foam were installed in the base plate: inline, corrugated, and zigzag; Fig. 3 depicts exaggerated sketches of each foam configuration. The inline and corrugated configurations were designed based on specifications.[‡] The proposed advantage to

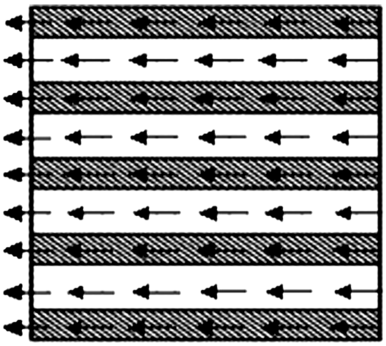

a) Inline configuration

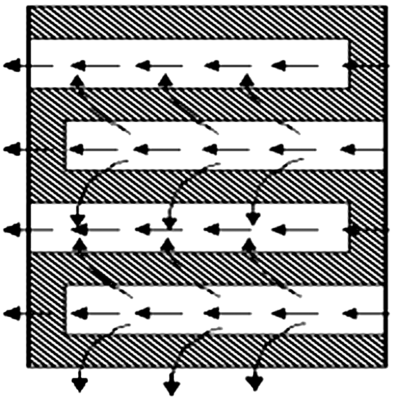

b) Corrugated configuration

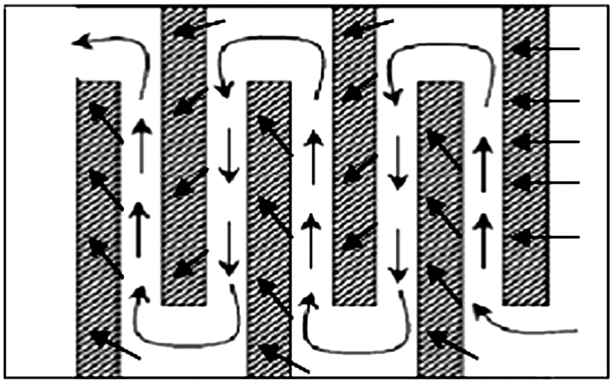

c) Zigzag configuration

Fig. 3 Graphite-foam configurations.

using these foams is that the porosity of the foam provides an increased amount of surface area to convectively interact with the fluid in the cooling channel. It is the goal of the current study to experimentally evaluate graphite foam with water cooling and determine how much the foam enhances the heat transfer with water cooling, as compared with air [12] cooling, and which configuration provides the best performance for the present application. The nanoparticles Al_2O_3 and CuO were obtained from Meliorum[§], with both types of particles sized at a 40 nm diameter.

III. Experimental Procedure

Before the fabrication of the experimental test apparatus, CFD simulations were conducted using IcePak, a CFD software package from Fluent, Inc., to simulate and guide the experimental setup.

[‡]Personal communication with J. Klett of ORNL, September 2004.

[§]Data available online at http://www.meliorum.com [retrieved December 2006].

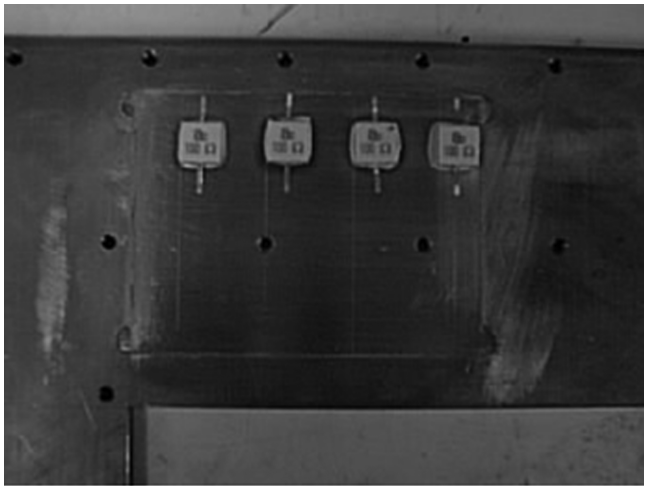

Fig. 4 Base plate with chip resistors.

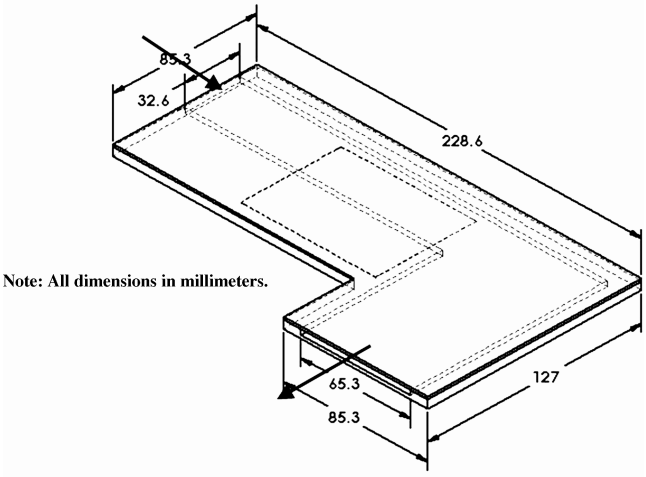

Fig. 5 Water-cooled base-plate sketch.

Initially simulations were conducted with and without modeling the effects of radiation. Results showed that due to the significant convective air flow through the cabinet, the radiation effects were negligible. These CFD simulations revealed that of the seven chips (see Fig. 1) that populate the power-amplifier unit, only the power chip exhibits a significant impact on the unit temperature; thus, for the experimental testing, only the power-amplifier chip was simulated. It was also determined from the CFD simulations that the chip temperatures of the units on one stick are essentially independent of the chip temperatures on adjacent sticks. This allowed for only one stick to be simulated experimentally. However, the other sticks were replaced with dummy sticks made of Plexiglas to maintain the integrity of the flowfield and to preserve the packing spacing of 0.020 m mentioned earlier. These modifications resulted in faster experimental hardware buildup and improved the experimental quality.

Figure 4 is a photograph of the base plate with the cover removed, exposing the power chips. A 100Ω ($\pm 0.5\Omega$) chip resistor manufactured by American Technical Ceramics (LR13737T0100J) was used to simulate the power chip. The dimensions and material architecture of this resistor ($9.4 \times 9.4 \times 1.87$ mm) are similar to that expected for a realistic power-amplifier chip; the details of the chip architecture are contained in Table 1.

The base plate was fabricated in two sections to facilitate easy access to the cooling channel. The primary section of the base plate, referred to as the top, is 4.76 mm (0.188 in.) thick and has the chips mounted to one side and the cooling channel machined in the other side; it is fabricated from alloy 110 copper ($k = 391$ W/(m · °C)). Figure 5 details the dimensions of the base plate and cooling channel. The cooling channel is 32.6 mm wide with a height of 3 mm. The other part of the base plate, the bottom, is 1.59 mm (0.0625 in.) thick. Experimental tests were conducted with a bottom section made of Plexiglas so that the flow inside of the cooling channel could be visualized. The chips are located on the other side (top) of the base plate in the dashed area shown in Fig. 5.

The three different geometrical configurations (inline, corrugated, and zigzag) of graphite foam that were investigated are illustrated in Fig. 6. For each of these configurations, POCO foam and POCO HTC foam were tested. The POCO foam has a thermal conductivity

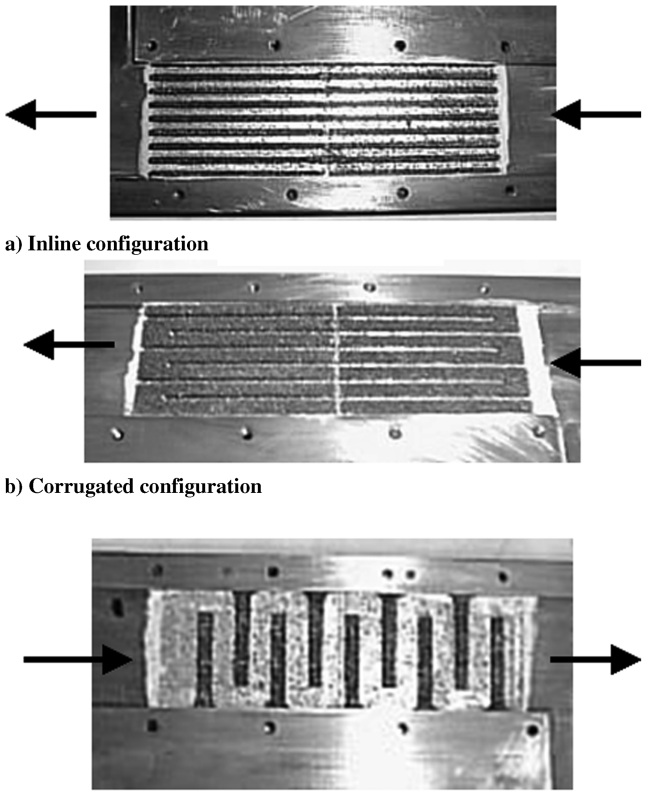

a) Inline configuration

b) Corrugated configuration

c) Zigzag configuration

Fig. 6 Graphite-foam configurations in the cooling channel.

of 135 W/(m · °C) in the downward direction and a total porosity of 75%; the POCO HTC foam has a thermal conductivity of 245 W/(m · °C) in the downward direction and a total porosity of 61%.[¶] Both a high thermal conductivity and a high porosity are desirable, but these two properties are counter to one another. A high

Table 1 Material properties of chip resistor used to simulate the power-amplifier chip

Chip layer	Material	Thickness, mm	k, W/(m · °C)	Density, kg/m^3	Specific heat, J/(kg · °C)
Substrate	AlNi	1.02	170	3970	910
Resistive element	Tantalum	0.55	57.5	16650	153
Cover	Alumina	0.30	27	3260	740

[a]Chip base area is 9.4×9.4 mm.

[¶]Data available online at http://www.poco.com [retrieved October 2006].

Table 2 Graphite-foam and copper-fin configurations specifications

Configuration	Fin thickness, mm	Spacing, mm	Fin length, mm	No. of fins
Inline	1.6	2.4	97	9
Corrugated	3.2	1.6	97	7
Zigzag	3.7	6.4	26	9

thermal conductivity draws the heat from the base plate into the cooling channel more quickly. A high porosity allows more surface area for convectively drawing the heat from the foam and into the cooling fluid.

For the zigzag and inline configurations, experiments were conducted in which the fins were also made of copper instead of graphite foam for comparison purposes. All of the configurations have a fin height of 3 mm. The dimensions (thickness and length) of the fins for the inline and corrugated configurations were based on directives from ORNL (footnote [‡]). Table 2 contains the dimensional specifications for the various cooling configurations. The fins for the inline configuration have a thickness of 1.6 mm and are separated by a gap of 2.4 mm. The corrugated configuration has a fin thickness of 3.2 mm with a gap between fins of 1.6 mm (footnote [‡]). The fins for the zigzag configuration have a thickness of 3.7 mm separated by a gap of 6.4 mm; for the zigzag cooling configuration, a fin is placed directly below a chip resistor mounted on the opposite side of the base plate. Also, based on CFD predictions, the zigzag fins were made to a length of 80% (26 mm) of the cooling-channel width. Figure 7 shows the cooling channel with a sample of the copper zigzag fins installed. For all configurations (footnote [‡]), the material was held in place with a silver-loaded epoxy (DM6030HK) obtained from Diemat, Inc. This epoxy has a very high thermal conductivity (60 $W/(m \cdot °C)$) as compared with other epoxies and adhesives.

The Al_2O_3 particles [15] have a density of 3970 kg/m^3, a thermal conductivity of 36 $W/(m \cdot °C)$, and a size of 40 nm in diameter. The CuO particles (footnote [§]) [16] have a density of 6000 kg/m^3, a thermal conductivity of 20 $W/(m \cdot °C)$, and a size of 40 nm in diameter. The particle concentrations (by volume) were varied from 0% up to a maximum of 7%.

Figure 8 shows the experimental apparatus for the water-cooled base plate incorporating a pump, expansion tank, and heat exchanger. The water travels through a manifold before entering and after exiting the base plate. Ten sheets of nylon screen with a mesh size of 1.8 mm and a wire diameter of 0.25 mm were inserted into the manifold to ensure a uniform flowfield inside the cooling channel. The pump, which was manufactured by Little Giant Company (977409), was used to circulate the water through the base-plate cooling channel. The heat exchanger, manufactured by Lytron (M05-050SB1), was implemented to remove the heat from the cooling fluid before recirculating the water. An Omega acrylic rotameter (FL7301) was used to monitor the flow rate through the cooling channel; this rotameter has an accuracy of 6% full scale and a repeatability of 1% full scale. The nanoparticles were monitored in the expansion tank (Fig. 8) to confirm that the particles remained in suspension.

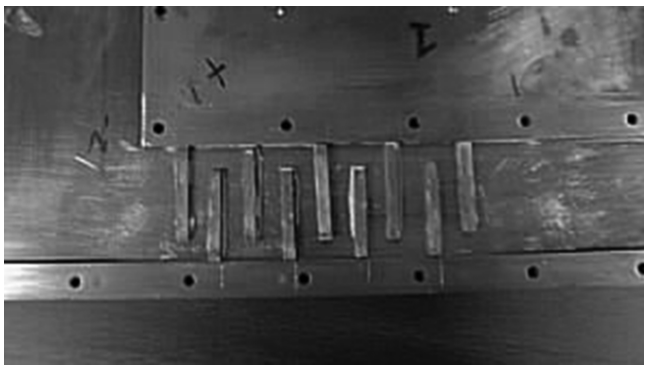

Fig. 7 Stick with copper zigzag fins in the cooling channel.

Power for the chips was supplied by two variable-dc power supplies. Two digital multimeters were used to accurately monitor the voltage (Fluke 37) and current (Fluke 8010A) being supplied to the chips. The temperature at the top of each power chip was measured with type-J thermocouples (±0.5°C) and recorded using a data acquisition system (HP VEE). Experiments were conducted with thermal-dissipation power levels of 20 W (±0.13 W), 30 W (±0.18 W), and 42 W (±0.25 W) input into the system. Having described the experimental setup and procedure, the results from this study will be presented in the next section.

IV. Results

The data shown in Figs. 9–19 represent the steady-state temperatures of the power chips at the different levels of dissipated thermal power and volume flow rates of fluid in the cooling channel, both with and without nanoparticles and both with and without a variety of inserts into the cooling channel to enhance the heat transfer and hence reduce the power-chip temperatures. The term *water only* means a water-only open channel for all figures (Figs. 9–19) in the results. The inlet water temperature remained essentially constant at

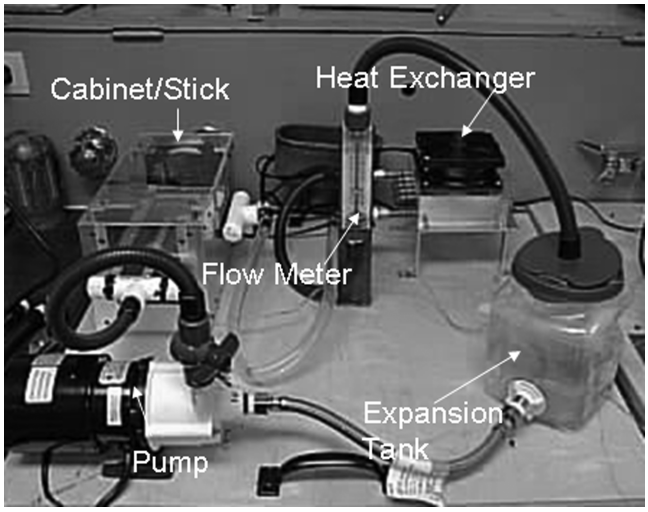

Fig. 8 Water-cooling flow circuit setup.

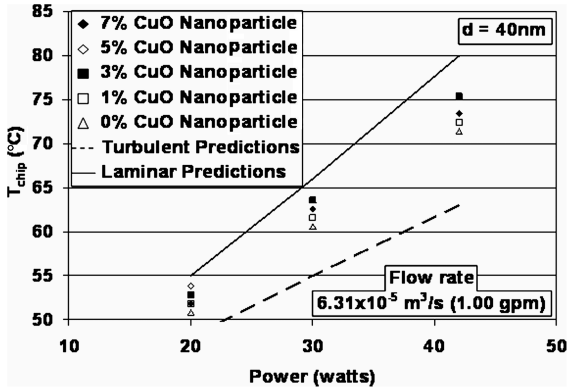

Fig. 9 Comparison of percent volume concentration for CuO nanoparticles to Icepak water-only predictions for 6.31×10^{-5} m^3/s flow rate and $T_\infty = 25°C$.

about 32°C and the heat exchanger was adequate at maintaining this temperature throughout the duration of the experiments. Data are expressed in terms of power-chip temperature as a function of dissipated thermal power. All water-cooling experimental data and CFD predictions illustrate a linear behavior, as did the air-cooling CFD predictions and experimental data of [12]; this can be very beneficial in predicting power-chip temperatures at other power levels and at other ambient-temperature environments. The numerical-model grid was made successively finer until the predictions were grid-independent.

Three base plates were fabricated to expedite the experimental process. Different base plates were used for the various geometric configurations (inline, corrugated, zigzag, and nanoparticles). Before inserting any graphite-foam or copper material into the

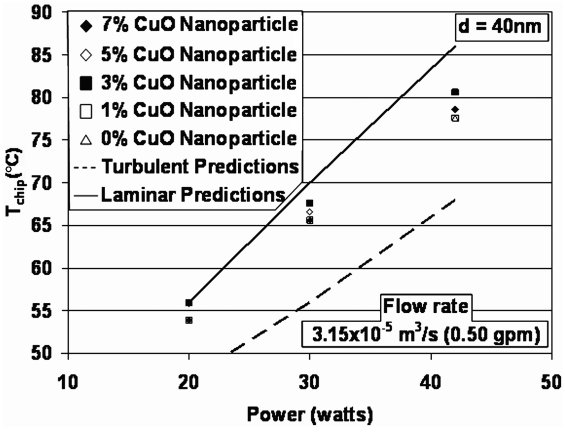

Fig. 10 Comparison of percent volume concentration for CuO nanoparticles to Icepak water-only predictions for 3.15×10^{-5} m^3/s flow rate and $T_\infty = 25$°C.

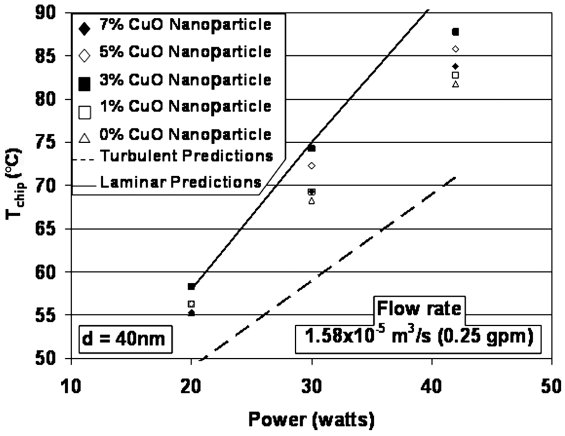

Fig. 11 Comparison of percent volume concentration for CuO nanoparticles to Icepak water-only predictions for 1.58×10^{-5} m^3/s flow rate and $T_\infty = 25$°C.

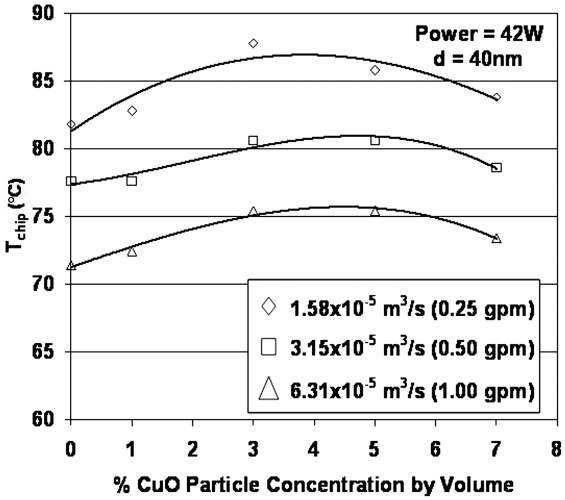

Fig. 12 Chip temperature at 42 W of power dissipation versus percent CuO nanoparticle concentration for $T_\infty = 25$°C.

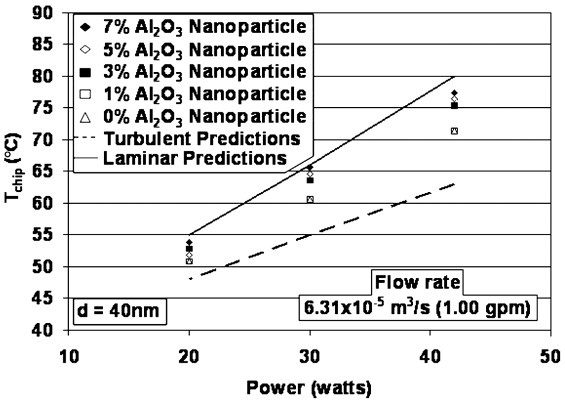

Fig. 13 Comparison of percent volume concentration for Al_3O_2 nanoparticles to Icepak water-only prediction for a flow rate of 6.31×10^{-5} m^3/s and $T_\infty = 25$°C.

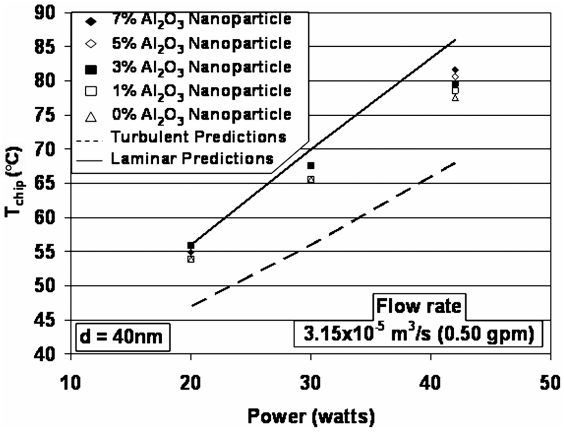

Fig. 14 Comparison of percent volume concentration for Al_3O_2 nanoparticles to Icepak water-only prediction for a flow rate of 3.15×10^{-5} m^3/s and $T_\infty = 25$°C.

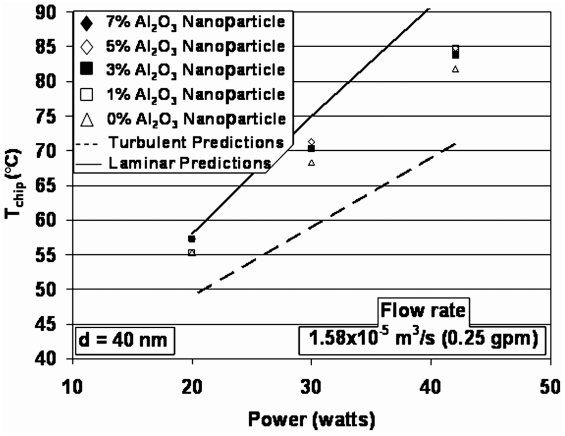

Fig. 15 Comparison of percent volume concentration for Al_3O_2 nanoparticles to Icepak water-only prediction for a flow rate of 1.58×10^{-5} m^3/s and $T_\infty = 25$°C.

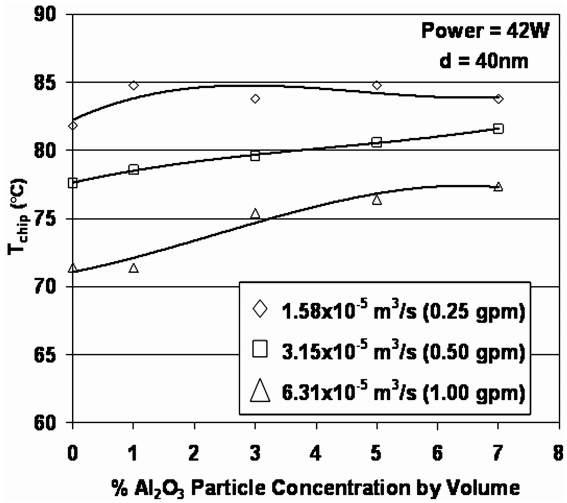

Fig. 16 Chip temperature at 42 W of power dissipation versus percent Al_2O_3 nanoparticle concentration for $T_\infty = 25°C$.

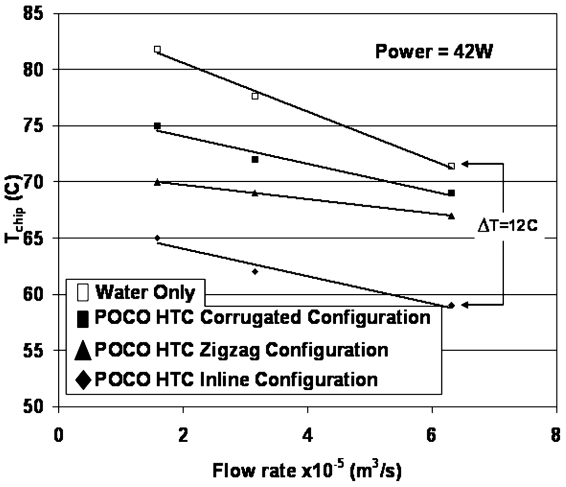

Fig. 18 Flow rate effect for POCO HTC foam with various configuration tested for water cooling, $T_\infty = 25°C$.

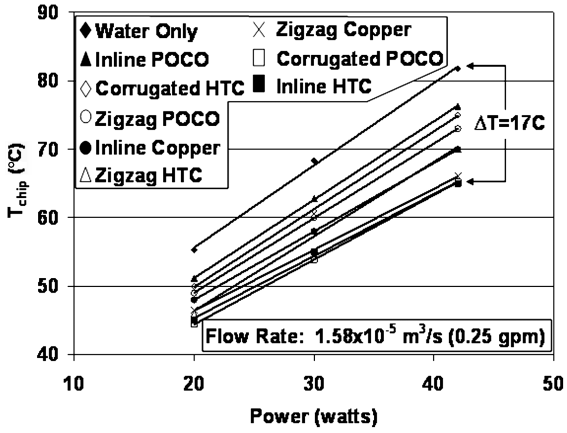

Fig. 17 Summary of water-cooling schemes for a 1.58×10^{-5} m^3/s flow rate, $T_\infty = 25°C$.

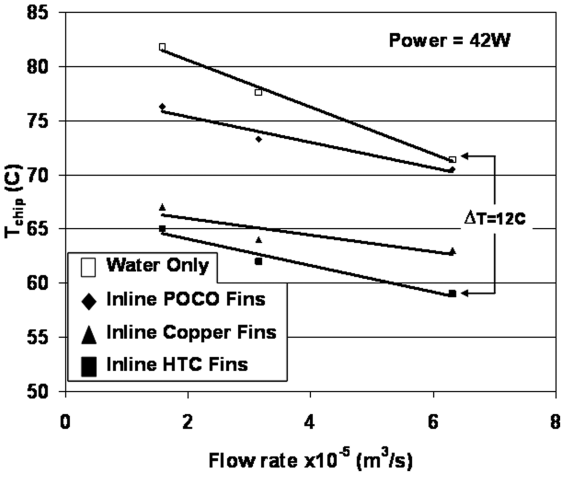

Fig. 19 Flow rate effect for an inline configuration with various fin material types tested for water cooling, $T_\infty = 25°C$.

cooling channel, data were obtained with water-only cooling to establish a baseline against which each of the enhancement inserts could be compared. Clearly, it is desired that any insert of graphite foam, copper fins, or nanoparticles would reduce the power-chip temperatures below the water-only baseline temperature values. All data were obtained at an ambient temperature T_∞ of 25°C.

A. CuO Nanoparticle Data

Das et al. [17] showed that the bulk thermal conductivity for a fluid with CuO nanoparticles and a fluid with Al_2O_3 nanoparticles increased by approximately 30% as the particle volume fraction was increased from 0 to 4%. This increase in thermal conductivity should result in some enhancement of the nanofluids' thermal performance, which, in this work, should yield some lowering of the power-chip experimental temperatures. Nguyen et al. [18] used a CFD model to predict the improvement in the effective convective heat transfer coefficient for an experimental configuration with flow rates similar to the experimental investigation presented here. The predictions in [18] indicated about a 60% increase in the effective convective heat transfer coefficient in the cooling channel. Employing the effective convective heat transfer coefficient values in [18] in our CFD model indicated that the power-chip temperatures should decrease by about 5°C as the nanoparticle volume concentration is increased from 0 to 7.5%; the experimental data in the present work correspond to varying the nanoparticle volume concentration from 0 to 7%.

The experimental results for CuO nanoparticles are shown in Figs. 9–12. The results in these figures demonstrated a surprising result in that the power-chip temperatures were measured to be higher than for the water-only (no particles, 0% volume concentration) case; however, this can be explained. The dashed lines in Figs. 9–11 show the CFD-predicted temperatures for water-only fully turbulent flow; the solid lines in Figs. 9–11 show the CFD-predicted power-chip temperatures for water-only fully laminar flow. These lines (dashed or solid) are not absolute boundaries for water-only fully turbulent flow and fully laminar flow, but do provide a reasonable prediction of the general range of power-chip temperatures between the two flow regimes. For the turbulent water-only predictions, both the Prandtl mixing-length model and the $\hat{k}$-ε model were used, with both resulting in temperatures within 1°C. The water-only (0% volume fraction) experimental-power-chip temperatures are seen to be between these two flow-regime approximate boundaries, thus indicating that the nature of the flow is in the transition region from laminar to turbulent; the flowfield in this work is in the hydraulic and thermal entrance regions. There are two strongly and oppositely competing phenomena to influence the convective heat transfer in the cooling channel:

1) The presence of the nanoparticles increases the bulk thermal conductivity of the fluid, which should help to lower the power-chip temperatures.

2) The presence of the nanoparticles in the fluid will act to dampen down disturbances within the flowfield and to hence push the flowfield to behave more like a laminar flowfield (thus less turbulent), with the impact of lowering the effective convective heat transfer coefficient (hence resulting in higher power-chip temperatures).

Thus, it seems from Figs. 9–11 that this (preceding phenomenon 2) indeed appears to be the case, with the nanoparticles pushing the overall flowfield nearer to the fully-laminar-type flow in the cooling channel. For the application under investigation, phenomenon 2 has a greater impact on the convective heat transfer. In other words, the change in the nature of the flow (caused by the nanoparticles) hinders the heat transfer more than the increase in bulk fluid thermal conductivity (caused by the nanoparticles) enhances the heat transfer.

Figure 12 depicts that the impact discussed already is not monotonic for CuO nanoparticles. Above a nanoparticle volume concentration of about 3%, the power-chip temperatures begin to decrease slowly again, but do not quite return down to the 0% nanoparticle concentration temperatures; this is because beyond about a 3% nanoparticle volume concentration, the increased bulk thermal conductivity of the fluid appears to begin to lower the power-chip temperatures. Thus, it appears that the CuO nanoparticles do not yield a net positive enhancement in lowering the power-chip temperatures as compared with the water-only (0% volume concentration) case; this is because the cooling-channel flow is in the transitional regime before the nanoparticles are inserted into the fluid flowfield.

B. Al_2O_3 Nanoparticle Data

To confirm the preceding results, the experimental test was repeated with Al_2O_3 nanoparticles. These particles have a higher thermal conductivity but a lower density than the CuO nanoparticles. The higher thermal conductivity should help increase the fluid thermal conductivity, but the lower bulk density should lessen the dampening effect on influencing the flow toward behaving more laminar in nature. Figures 13–15 for the Al_2O_3 nanoparticles show a similar behavior to that contained in Figs. 9–11 for the CuO nanoparticles. Namely, the dampening by the nanoparticles of the disturbances in the flowfield is more dominant and causes the nature of the flow to behave more nearly laminar and hence reduces the convective heat transfer in the cooling channel. Again, all of the power-chip temperature data with nanoparticles were higher than the water-only (0% volume concentration) data.

The results shown in Fig. 16 for the Al_2O_3 nanoparticles illustrate somewhat of a similar type of behavior as for the CuO nanoparticles in Fig. 12, except at a 7% volume concentration the power-chip temperatures have not yet begun to decrease significantly but do appear to be leveling off. However, the overall net impact is to cause the power-chip temperatures to increase as a result of the nanoparticles, causing the flowfield to behave more laminar in nature.

C. Graphite-Foam Data

A comparison of the geometric configurations of foam and copper inserts tested is shown in Fig. 17. The inline POCO HTC foam, zigzag copper, and corrugated POCO foam configurations all showed similar best performances (at 42 W) by reducing the chip temperature by about 17°C for the low flow rate as compared with the water-only cooling. Problems may occur with the corrugated POCO essentially acting as a filter and becoming clogged over time. The zigzag copper configuration requires more pumping power due to a higher pressure drop through the cooling channel; therefore, the inline POCO HTC appears to be best because it has equally good performance but does not have the application difficulties associated with the other two configurations.

Shown in Figs. 18 and 19 is the flow rate effect for the different fin-insert configurations. Because the POCO HTC foam was shown to have the best performance in Fig. 17, the POCO HTC foam was selected to illustrate the flow rate effect for the three geometric configurations tested. Figure 18 shows that by increasing the flow rate, an additional improvement of about 7°C can be achieved over the results shown in Fig. 17 at 42 W of power dissipation. Figure 19 depicts the impact of flow rate by selecting a specific geometric configuration (inline) and comparing the various fin materials. Again, the POCO HTC foam is seen to be the best performer and an additional 7°C of thermal performance can be achieved as a function of flow rate

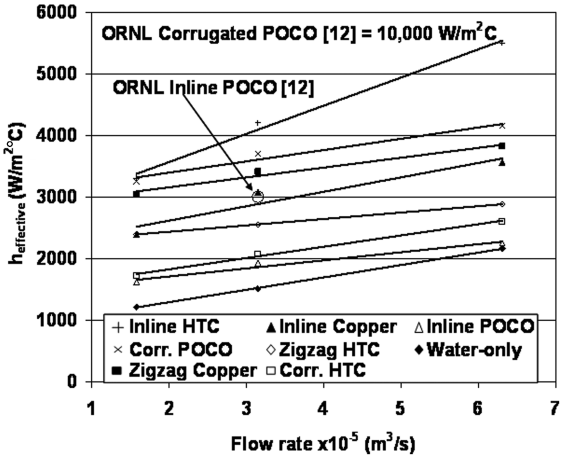

Fig. 20 Effective heat transfer coefficient for various water-cooled configurations at a power dissipation of 42 W, $T_\infty = 25$°C.

In association with Fig. 17, Fig. 20 contains the effective convective heat transfer coefficients for the various configurations tested, along with the estimated values from ORNL (footnote [‡]). These effective heat transfer coefficients were reverse-engineered using the IcePak software. This provides a magnitude comparison of the results here with that of ORNL values. The effective convective heat transfer coefficients were determined by using IcePak and the experimental temperature data. This was done by inserting a convective heat transfer coefficient value into the CFD model and varying it until the temperatures from the CFD model matched the temperatures from the experimental data. It can be seen in Fig. 20 that the ORNL estimate for the inline POCO configuration is of the same magnitude as those reverse-engineered for the current study; however, the ORNL estimate for the corrugated POCO configuration is much higher. The foam thickness (0.003 m) employed in the present investigation was significantly different from the foam thickness used in the ORNL testing, which could explain the difference in the effective heat transfer coefficients.

The goal of the current study was to maintain temperatures below the failure temperature of 150°C for a dissipated power level of 42 W, even in harsh desert conditions in which the ambient temperature could be as high as 50°C. Results from IcePak simulations show that the power-amplifier temperatures will shift by the amount of change in the ambient temperature from 25°C. Assuming that the CFD predictions are accurate, the power-chip temperatures would remain below the failure temperature of 150°C for all of the configurations tested if the curves in all of the figures were shifted upward by 25°C (desert conditions). However, the better-performing cooling-channel inserts would permit even much higher heat-dissipation levels in the power chips before reaching the failure temperature of 150° C, even at desert conditions. For example, the inline POCO HTC from Fig. 17 would allow a thermal heat dissipation of approximately 125 W before nearing the failure temperature of 150°C at desert conditions ($T_\infty = 50$°C).

V. Conclusions

The CuO and Al_2O_3 nanoparticle results in this work showed surprising results in that the power-chip temperatures were increased by the presence of both particle types, and hence the use of nanoparticles is not recommended for thermal-management applications similar to the overall configuration explored in this work.

The graphite-foam results obtained in this work illustrate that all of the cooling configurations evaluated did demonstrate some improvement over water-only cooling (no inserts). The order of performance measured, with 1 being the best, is as follows: 1) inline POCO HTC foam, 2) corrugated POCO foam, 3) zigzag copper fins,

4) inline copper fins, 5) zigzag POCO HTC foam, 6) zigzag POCO foam, 7) corrugated POCO HTC foam, 8) inline POCO foam, and 9) water only (no insert in the cooling channel).

In general, all of the inserts proved to have a strong impact as mini heat exchangers. The best overall performance reduced the chip temperatures at 42 W of heat dissipation by about 17°C. It was also observed that increasing the flow rate in the cooling channel resulted in lower power-chip temperatures. It is hoped that the experimental data presented here will help other researchers and designers in achieving thermal-management solutions in high-density-packing situations of electronic components.

References

[1] Azar, K., "Cooling Technology Options, Part 1," *Electronics Cooling*, Vol. 9, No. 3, Aug. 2003, pp. 10–14.

[2] Yeh, L. T., and Chu, R. C., *Thermal Management of Microelectronic Equipment*, American Society of Mechanical Engineers, New York, 2002.

[3] Chu, R. C., "The Challenges of Electronic Cooling: Past, Current, and Future," *Journal of Electronic Packaging*, Vol. 126, No. 4, 2004, pp. 491–500.
doi:10.1115/1.1839594

[4] Bar-Cohen, A., "Thermal Design and Control," *Chapter 9, Physical Architecture of VLSI Systems*, edited by R. J. Hannemann, A. D. Kraus, and M. Pecht, Wiley, New York, 1994, Chap. 9.

[5] Incropera, F. P., *Liquid Cooling of Electronic Devices by Single-Phase Convection*, Wiley, New York, 1999.

[6] Muwanga, R., and Hassan, I., "Flow and Heat Transfer in a Cross-Linked Silicon Microchannel Heat Sink," *Journal of Thermophysics and Heat Transfer*, Vol. 22, No. 3, 2008, pp. 333–341.
doi:10.2514/1.33952

[7] Yamamoto, H., Udagawa, H. Y., and Suzuki, M., "Cooling System for FACOM M-780 Large Scale Computer," *Cooling Technology for Electronic Equipment*, edited by W. Aung, Hemisphere, New York, 1988, pp. 701–730.

[8] Kishimoto, T., and Ohsaki, T., "VLSI Packaging Technique Using Liquid-Cooled Channels," *IEEE Transactions on Components, Hybrids, and Manufacturing Technology*, Vol. 9, No. 4, Dec. 1986, pp. 328–335.
doi:10.1109/TCHMT.1986.1136661

[9] Marotta, E. E., Ellsworth, M., and Mazzuca, S., "Thermal Performance of Silicon-Die/Water-Cooled Heat-Sink Assembly: Experimental Investigation," *Journal of Thermophysics and Heat Transfer*, Vol. 18, No. 2, 2004, pp. 193–202.
doi:10.2514/1.10175

[10] Garner, S. D., "Heat Pipes for Electronics Cooling Applications," *Electronics Cooling*, Vol. 2, No. 3, Sept. 1996.

[11] Bahrami, M., Yovanovich, M., and Culham, J., "Assessment of Relevant Physical Phenomena Controlling Thermal Performance of Nanofluids," *Journal of Thermophysics and Heat Transfer*, Vol. 21, No. 4, 2007, pp. 673–680.
doi:10.2514/1.28058

[12] Williams, Z. A., and Roux, J. A., "Graphite Foam Thermal Management of a High Packing Density Array of Power Amplifiers," *Journal of Electronic Packaging*, Vol. 128, No. 4, 2006, pp. 456–465.
doi:10.1115/1.2353282

[13] Klett, J., and Conway, B., "Thermal Management Solutions Utilizing High Thermal Conductivity Graphite Foams," *Proceedings of the 45th International SAMPE Symposium and Exhibition*, Society for the Advancement of Material and Process Engineering, Covina, CA, 2000, http://www.ornl.gov/~webworks/cpr/rpt/106741_.pdf [retrieved June 2004].

[14] Coursey, J. S., Kim, J., and Boudreaux, P. J., "Performance of Graphite Foam Evaporator for Use in Thermal Management," *Journal of Electronic Packaging*, Vol. 127, No. 2, 2005, pp. 127–134.
doi:10.1115/1.1871193

[15] Holman, J. P., *Heat Transfer*, 9th ed., edited by J. P., Holman, and J. Lloyd, Tata McGraw–Hill, New Delhi, India, 2004, pp. 597.

[16] Kwak, K., and Kim, C., "Viscosity and Thermal Conductivity of Copper Oxide Nanofluid Dispersed in Ethylene Glycol," *Korea-Australia Rheology Journal*, Vol. 17, No. 2, June 2005, pp. 35–40.

[17] Das, S. A., Putra, N., Thiesen, P., and Roetzel, W., "Temperature Dependence of Thermal Conductivity Enhancement for Nanofluids," *Journal of Heat Transfer*, Vol. 125, No. 4, Aug. 2003, pp. 567–574.
doi:10.1115/1.1571080

[18] Nguyen, C. T., Roy, G., Maiga, S. E., and Lajoie, P. R., "Heat Transfer Enhancement by Using Nanofluids for Cooling of High Heat Output Microprocessor," *Electronic Cooling*, Vol. 10, No. 4, Nov. 2004, pp. 38–40.